

# PI4KIII $\beta$ Activity Regulates Lateral Root Formation Driven by Endocytic Trafficking to the Vacuole<sup>1</sup>

Carlos Rubilar-Hernández, Claudio Osorio-Navarro, Francisca Cabello, and Lorena Norambuena<sup>2,3</sup>

Plant Molecular Biology Centre, Department of Biology, Faculty of Sciences, Universidad de Chile, Santiago, Chile

ORCID IDs: 0000-0002-4561-8539 (C.R.-H.); 0000-0002-0589-3392 (C.O.-N.); 0000-0002-5356-9968 (F.C.); 0000-0002-6031-2394 (L.N.).

Lateral roots (LRs) increase the contact area of the root with the rhizosphere and thereby improve water and nutrient uptake from the soil. LRs are generated either via a developmentally controlled mechanism or through induction by external stimuli, such as water and nutrient availability. Auxin regulates LR organogenesis via transcriptional activation by an auxin complex receptor. Endocytic trafficking to the vacuole positively regulates LR organogenesis independently of the auxin complex receptor in *Arabidopsis* (*Arabidopsis thaliana*). Here, we demonstrate that phosphatidylinositol 4-phosphate (PI4P) biosynthesis regulated by the phosphatidylinositol 4-kinases PI4KIII $\beta$ 1 and PI4KIII $\beta$ 2 is essential for the LR organogenesis driven by endocytic trafficking to the vacuole. Stimulation with Sortin2, a biomodulator that promotes protein targeting to the vacuole, altered PI4P abundance at both the plasma membrane and endosomal compartments, a process dependent on PI4K activity. These findings suggest that endocytic trafficking to the vacuole regulated by the enzymatic activities of PI4KIII $\beta$ 1 and PI4KIII $\beta$ 2 participates in a mechanism independent of the auxin complex receptor that regulates LR organogenesis in *Arabidopsis*. Surprisingly, loss-of-function of PI4KIII $\beta$ 1 and PI4KIII $\beta$ 2 induced both LR primordium formation and endocytic trafficking toward the vacuole. This LR primordium induction was alleviated by exogenous PI4P, suggesting that PI4KIII $\beta$ 1 and PI4KIII $\beta$ 2 activity constitutively negatively regulates LR primordium formation. Overall, this research demonstrates a dual role of PI4KIII $\beta$ 1 and PI4KIII $\beta$ 2 in LR primordium formation in *Arabidopsis*.

Lateral roots (LRs) are postembryonic organs that increase the surface area of the root and expand the territory for the uptake of water and nutrients from the soil. LR organogenesis is achieved by a developmental program that generates a new organ within the primary root (Malamy and Benfey, 1997). Near the tip of the primary root, specific cells of the pericycle cell layer are specified as LR founder cells. LR founder cells divide asymmetrically, generating a LR primordium (LRP). The LRP increases in size and cell number until it crosses the outer primary root layer, at which point it constitutes an emerged LR (eLR; Casimiro et al., 2001; Petricka et al., 2012). Plant roots constantly and regularly generate new LRs as part of a developmentally controlled mechanism (Van Norman et al., 2013). LR organogenesis can also be stimulated by environmental

factors, thereby modifying root system architecture according to growth conditions (Lima et al., 2010; Gruber et al., 2013).

The phytohormone auxin is a key regulator of LR organogenesis (Boerjan et al., 1995; Casimiro et al., 2001; Dubrovsky et al., 2008; Marhavý et al., 2013). In *Arabidopsis* (*Arabidopsis thaliana*), auxin is perceived by the F-box auxin receptors *transport inhibitor resistant1/Auxin signaling F box proteins* (TIR1/AFB), comprising part of the E3 ubiquitin-ligase SKP, Cullin, F-box (SCF)<sup>TIR1/AFB</sup> complex (Dharmasiri et al., 2005; Kepinski and Leyser, 2005). This activates an auxin-dependent transcriptional response that leads to the formation of LRPs (Fukaki et al., 2005; Okushima et al., 2007; Dubrovsky et al., 2008; De Rybel et al., 2010; Xuan et al., 2015). The regulation of both auxin perception and auxin-dependent transcriptional activation plays important roles in this developmental process in response to various stimuli (Pérez-Torres et al., 2008; Miura et al., 2011; Li et al., 2015).

An alternative molecular pathway to the SCF<sup>TIR1/AFB</sup>-dependent mechanism is also present in *Arabidopsis*, but the underlying molecular mechanism has not been elucidated. LR organogenesis can occur independently of the auxin receptor TIR1 when the primary root is mechanically stimulated or exposed to Glc (Mishra et al., 2009; Richter et al., 2009; Zolla et al., 2010). In addition, treatment with the synthetic chemical compound Sortin2, which affects membrane and protein targeting to the vacuole, induces LR organogenesis driven by a mechanism independent of

<sup>1</sup>This work was supported by Fondecyt (grant nos. 1120289 and 1170950); VID Enlace (grant no. 2016 ENL015/16 from Universidad de Chile); and Conicyt (PhD fellowship and grant no. 21120545 to C.R.-H.).

<sup>2</sup>Author for contact: lnorambuena@uchile.cl.

<sup>3</sup>Senior author.

The author responsible for distribution of materials integral to the findings presented in this article in accordance with the policy described in the Instructions for Authors ([www.plantphysiol.org](http://www.plantphysiol.org)) is: Lorena Norambuena (lnorambuena@uchile.cl).

C.R.-H., C.O.-N., and F.C. performed the experiments; C.R.-H. and L.N. designed the experiments, analyzed the data, and wrote the paper.

[www.plantphysiol.org/cgi/doi/10.1104/pp.19.00695](http://www.plantphysiol.org/cgi/doi/10.1104/pp.19.00695)

SCF<sup>TIR1/AFB</sup> without affecting the transcriptional response related to auxin perception (Pérez-Henríquez et al., 2012).

We previously demonstrated that the effect of Sortin2 is due to the induction of endocytic trafficking to the vacuole (Pérez-Henríquez et al., 2012; Vásquez-Soto et al., 2015). In this type of trafficking pathway, components at the plasma membrane are internalized to intracellular compartments as the trans-Golgi network/early endosome (TGN/EE) and late endosomes, which ultimately fuse with the vacuole. Inhibition of endocytic trafficking to the vacuole by treatment with the drug wortmannin reduces the stimulating effects of Sortin2 on LR organogenesis (Pérez-Henríquez et al., 2012). Notably, wortmannin does not affect LR organogenesis driven by the developmentally controlled mechanism (Emans et al., 2002; Beck et al., 2012; Pérez-Henríquez et al., 2012), reinforcing the role of endocytic trafficking in a distinctive molecular pathway leading to LR formation.

Wortmannin inhibits the enzymatic activities of phosphatidylinositol 3-kinase (PI3K) and phosphatidylinositol 4-kinase (PI4K; Matsuoka et al., 1995; Delage et al., 2012; Okazaki et al., 2015). PI3K and PI4K catalyze the formation of phosphatidylinositol 3-phosphate (PI3P) and PI4P from phosphatidylinositol, respectively. Therefore, the induction of LR formation by Sortin2 could depend on the activities of these types of phosphatidylinositol kinases. Both PI3P and PI4P are enriched in different compartments of the Arabidopsis endomembrane system (Simon et al., 2014) and are involved in several secretory and endocytic trafficking pathways (Kim et al., 2001; Preuss et al., 2006; Lee et al., 2008; Kang et al., 2011; Kolb et al., 2015).

Arabidopsis contains 12 putative PI4K-encoding genes in three gene families, *PI4K $\alpha$* , *PI4K $\beta$* , and *PI4K $\gamma$*  (Mueller-Roeber and Pical, 2002). The biological functions of only three of these genes (*PI4KIII $\alpha$ 1*, *PI4KIII $\beta$ 1*, and *PI4KIII $\beta$ 2*) have been elucidated (Delage et al., 2012; Heilmann and Heilmann, 2015; Okazaki et al., 2015). *PI4KIII $\alpha$ 1* is thought to be the main contributor to the PI4P levels required for chloroplast biogenesis in leaves (Okazaki et al., 2015), whereas *PI4KIII $\beta$ 1* and *PI4KIII $\beta$ 2* play redundant roles in root tissue (Preuss et al., 2006). Moreover, PI4K might function in endocytosis in primary roots (Fujimoto et al., 2015). Consistently, PI4P is primarily enriched at the plasma membrane and the TGN/EE in Arabidopsis root cells (Munnik and Nielsen, 2011; Simon et al., 2014). The loss of function of *PI4KIII $\beta$ 1* and *PI4KIII $\beta$ 2* impairs TGN/EE morphology and trafficking between the TGN/EE and the plasma membrane (Preuss et al., 2006; Kang et al., 2011). At the physiological level, both *PI4KIII $\beta$ 1* and *PI4KIII $\beta$ 2* regulate primary root growth and root hair polarity. However, there is currently no evidence linking PI4K activity or PI4P to LR organogenesis.

In this study, we demonstrate that PI4K activity is crucial for LRP formation promoted by the induction of endocytic trafficking. We demonstrate that *PI4KIII $\beta$ 1* and *PI4KIII $\beta$ 2* are essential for Sortin2-induced LRP

formation due to their role in PI4P synthesis. On the other hand, *PI4KIII $\beta$ 1* and *PI4KIII $\beta$ 2* constitutively repress LR organogenesis by functioning as negative regulators of endocytic trafficking. Overall, this study indicates that endocytic trafficking to the vacuole mediates root branching via a mechanism that depends on the activities of both *PI4KIII $\beta$ 1* and *PI4KIII $\beta$ 2* in Arabidopsis.

## RESULTS

### PI4K Activity Is Required for the Induction of Endocytic Trafficking and LRP Formation Stimulated by Sortin2

To explore the role of PI4K in LR organogenesis induced by endocytic trafficking to the vacuole, we evaluated the responses of seedlings to the PI4K inhibitor phenylarsine oxide (PAO; Simon et al., 2016). Seedlings (7 d old) were treated with different doses of PAO for 3 d. Treatment with 20  $\mu$ M PAO abolished the induction of LRP formation by Sortin2 (Fig. 1A). Similar concentrations of PAO have been used to abolish PI4K activity in foliar and radicular plant tissue (Okazaki et al., 2015; Simon et al., 2016). The induction of LRP formation induced by Sortin2 was also abolished by treatment with lower doses of PAO. Indeed, even the lowest concentration of PAO tested (0.1  $\mu$ M) inhibited

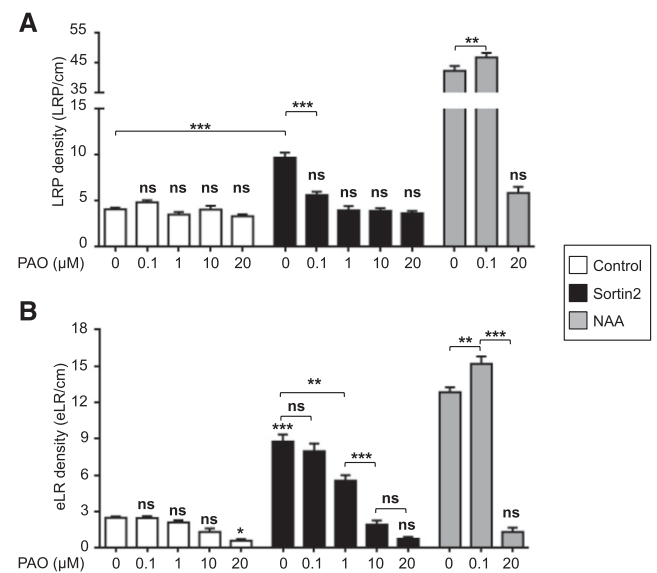


**Figure 1.** PI4K activity is required for the LRP formation induced by stimulated endocytic trafficking. Col-0 Arabidopsis seedlings (7 d old) were treated with MSL containing 58  $\mu$ M Sortin2 (black bars), 1% (v/v) dimethyl sulfoxide (DMSO; control, white bars), or 1  $\mu$ M NAA (gray bars) and coincubated with 0.1, 1, 10, or 20  $\mu$ M PAO. After 3 d, LRP (A) and eLR (B) density were scored. The experiments were performed at least in triplicate ( $n = 17$ –56 for control, 17–41 for Sortin2, and 11–36 for NAA). One-way ANOVA with Sidak's multiple comparisons test was performed: \*\*\* $P < 0.001$ ; \*\* $P < 0.01$ ; \* $P < 0.05$ ; ns (not significant;  $P > 0.05$ ) compared with control conditions (without both PAO and Sortin2) indicated above each bar or between conditions. Error bars denote SEM.

nearly 80% of Sortin2-induced LRP formation to a level comparable with that driven by the developmentally controlled mechanism (Fig. 1A).

By contrast, a 0.1  $\mu\text{M}$  PAO treatment did not inhibit LRP formation induced by the exogenous application of auxin 1-naphthaleneacetic acid (NAA; Fig. 1A). These results indicate that low doses of PAO specifically affect the LRP induction mechanism triggered by chemical stimulation with Sortin2. Remarkably, 0.1 to 10  $\mu\text{M}$  PAO failed to inhibit LRP establishment by the developmentally controlled mechanism, indicating that PAO-inhibited PI4K activity is dispensable for LRP formation driven by this mechanism (Fig. 1A). Notably, 20  $\mu\text{M}$  PAO inhibited NAA-induced LRP formation, suggesting that PI4K functions in auxin-induced LRP formation.

Furthermore, a 20  $\mu\text{M}$  PAO treatment inhibited LR emergence driven by the developmental program and by exogenous treatment with Sortin2 and NAA (Fig. 1B). These findings point to the presence of

a common PAO-targeted biological process distinct from the process targeted by 0.1  $\mu\text{M}$  PAO. Overall, these results strongly support the notion that PI4K activity plays a specific role in LRP formation driven by Sortin2-induced endocytic trafficking. Furthermore, these findings suggest that Sortin2 is an agonist of a molecular mechanism that is distinct from that driven by exogenous NAA treatment and the developmentally controlled mechanism to promote LRP formation.

Sortin2-induced LR formation is associated with an increased rate of endocytosis to the vacuole elicited by this compound (Pérez-Henríquez et al., 2012). Therefore, we evaluated the effect of inhibiting PI4K activity on endocytic trafficking by tracking the internalization of the endocytic tracer FM4-64 from the plasma membrane to the vacuole (Bolte et al., 2004; Tejos et al., 2018) over time in wild-type *Arabidopsis* root epidermal cells. Under control conditions, FM4-64 reached the endosomal compartments within 30 min and was detected in the vacuole membrane within 90 min

**Figure 2.** Inhibition of PI4K activity impairs the acceleration of endocytic trafficking to the vacuole required for LRP formation. A and B, Effect of PAO on endocytic trafficking induced by Sortin2. Col-0 seedlings (7 d old) were preincubated in MSL with 0.1  $\mu\text{M}$  PAO for 60 min (B). Mock conditions (without PAO) were included for comparison (A). The seedlings were subsequently incubated in 5  $\mu\text{M}$  FM4-64 at 4°C. After 5 min, 1% (v/v) DMSO (control) or 58  $\mu\text{M}$  Sortin2 (Sortin2; final concentration) was added and the seedlings were transferred to 22°C (Time 0). PAO levels were maintained at 0.1  $\mu\text{M}$  throughout the assay. FM4-64 internalization was evaluated for 120 min. Representative confocal single images corresponding to 5, 30, 60, 90, and 120 min of tracer internalization are shown. Scale bars = 10  $\mu\text{m}$ . Arrowheads indicate FM4-64-stained tonoplast. C, Trafficking to the vacuole evaluated under all conditions described in A and B. Epidermal root cells from independent primary roots displaying FM4-64-stained tonoplast were quantified. Mock treatment:  $n = 74$  to 143 cells for the control (7–9 roots);  $n = 107$  to 168 cells in Sortin2 (13–17 roots). Treated with PAO,  $n = 168$  to 267 cells for the control (9–13 roots),  $n = 144$  to 381 cells in Sortin2 (12–25 roots). Results are expressed as the percentage of the evaluated cells  $\pm$  SEM. Two-way ANOVA with Sidak’s multiple comparisons test was performed. \*\*\* $P < 0.001$ ; \* $P < 0.05$ ; not significant (ns):  $P > 0.05$ .

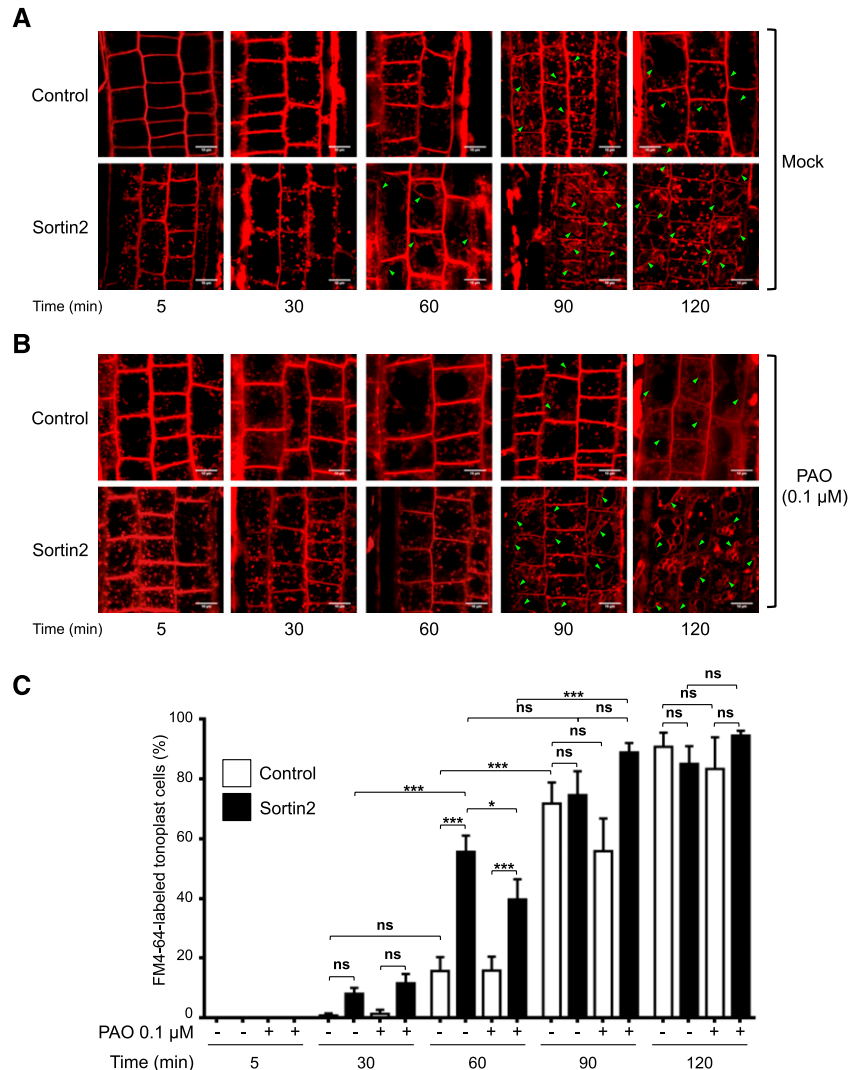




(Fig. 2A). As described by Pérez-Henríquez et al. (2012), upon Sortin2 treatment, endocytic trafficking occurred much more rapidly: FM4-64 reached the endosomes by 5 min and the tonoplast by 60 min (Fig. 2A). Indeed, after 60 min, FM4-64 reached the tonoplast in  $55.6\% \pm 5.4\%$  (SE) of cells in seedlings exposed to Sortin2, whereas under control conditions, only  $15.8\% \pm 4.7\%$  of cells displayed FM4-64-stained tonoplasts (Fig. 2C).

Treatment with  $0.1 \mu\text{M}$  PAO significantly decreased the population of cells with FM4-64-stained tonoplasts (to only  $39.6\% \pm 6.8\%$ ) at 60 min in Sortin2-treated seedlings (Fig. 2, B and C). By contrast, under control conditions, neither endocytic trafficking nor the population of cells with FM4-64-stained tonoplasts was affected by  $0.1 \mu\text{M}$  PAO treatment (Fig. 2). This concentration of PAO likely impairs PI4K activity, partially inhibiting the effects of Sortin2 on endocytic trafficking to the vacuole.

To confirm the identity of the vacuole structures observed after 60 min of FM4-64 internalization in Sortin2-treated seedlings (Fig. 2A), we used FM1-43 to label the tonoplast (Bolte et al., 2004). The tonoplast was labeled with FM1-43 before starting the FM4-64 internalization

assay, which was performed under the conditions described above (Fig. 2). By 60 min, FM4-64 had reached the tonoplast in Sortin2-treated seedlings, whereas in the control, very little FM4-64 was detected in this compartment (Fig. 3A, intensity map).

Consistently, plasma membrane-localized FM4-64 was less abundant in Sortin2-treated seedlings than in the control, suggesting that Sortin2 affects endocytic trafficking to the vacuole (Fig. 3A, yellow arrowheads). Under this condition, both tracers colocalized to the tonoplast, as revealed in the FM1-43/FM4-64 merged image (Fig. 3A). However, PAO inhibited the Sortin2-induced delivery of FM4-64 to the tonoplast (Fig. 3A, Sortin2+PAO). By a later time point (120 min), FM4-64 had reached the tonoplast under both Sortin2 and control conditions, but FM4-64 levels appeared to be higher in Sortin2-treated seedlings (Fig. 3B). These results strongly support the notion that Sortin2 induces endocytosis of the plasma membrane to the vacuole.

However,  $20 \mu\text{M}$  PAO completely blocked the internalization of the endocytic tracer from the plasma membrane in both control and Sortin2-treated seedlings (Supplemental Fig. S1), suggesting that PI4K plays

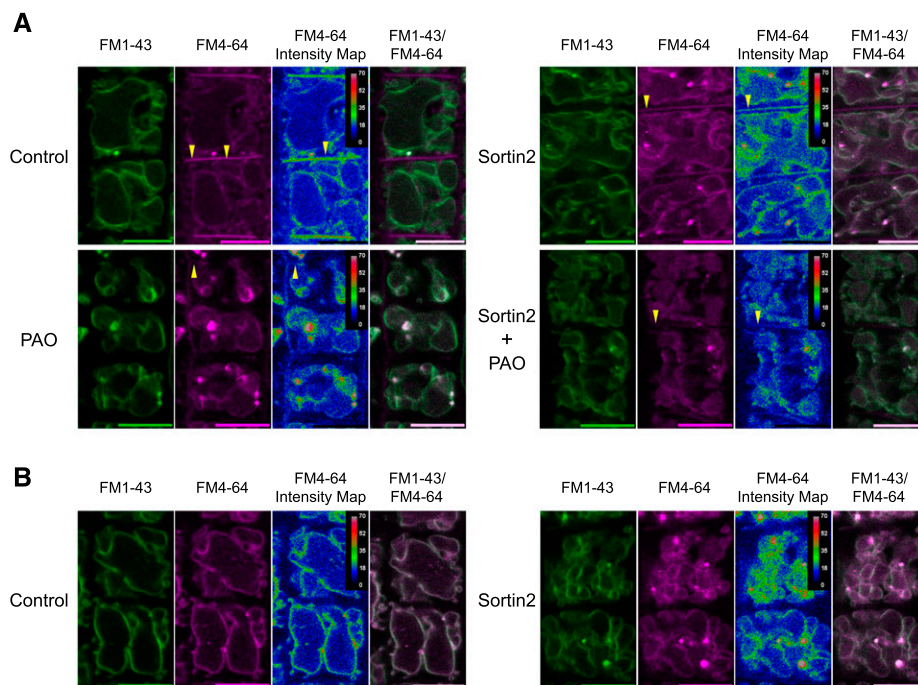


**Figure 3.** Inhibition of PI4K activity by PAO impairs Sortin2-stimulated trafficking of FM4-64 to the vacuole. Col-0 seedlings (7 d old) were incubated in  $5 \mu\text{M}$  FM1-43 for tonoplast labeling (green images). Seedlings were treated with  $0.1 \mu\text{M}$  PAO or 1% (v/v) DMSO (control) for 60 min. The seedlings were subsequently transferred to MSL supplemented with  $0.1 \mu\text{M}$  PAO,  $58 \mu\text{M}$  Sortin2,  $0.1 \mu\text{M}$  PAO plus  $58 \mu\text{M}$  Sortin2 (Sortin2+PAO), or control conditions, followed by the evaluation of FM4-64 internalization (magenta images). Confocal single images were taken at 60 (A) and 120 (B) min of FM4-64 internalization. Representative images from three independent experiments are shown. The fluorescence of FM4-64 is represented as an intensity map according to the scale included in each image. Images of tonoplasts colabeled with FM1-43 and FM4-64 are also shown. Codistribution of the tracers was analyzed in 12 roots by analyzing 10 cells per root for each experimental condition. Yellow arrowheads indicate the plasma membrane. Scale bars =  $10 \mu\text{m}$ .

a general role in endocytic trafficking. Furthermore, 20  $\mu\text{M}$  PAO-sensitive PI4K appears to contribute to the emergence of LR independently of the mechanism underlying LR organogenesis (i.e. the developmentally controlled program or that triggered by Sortin2 or NAA application; Fig. 1B).

Overall, these results point to the existence of at least two types of PI4K activities that differ in their sensitivity to PAO. PI4K activity sensitive to submicromolar concentrations of PAO contributes to Sortin2-induced endocytic trafficking to the vacuole and LRP formation.

### LRP Formation Driven by Endocytic Trafficking Requires PI4P Biosynthesis

Because PI4K activity is relevant for the LRP formation promoted by the chemical induction of endocytic trafficking, we reasoned that the levels or subcellular localization of PI4P would be altered after Sortin2 treatment. To monitor *in vivo* changes in PI4P, we evaluated the subcellular distribution of the PI4P biosensor yellow fluorescent protein (YFP)-PH<sup>FAPP1</sup> in an Arabidopsis transgenic line (Thole and Nielsen, 2008). This biosensor comprises YFP fused to a specific PI4P binding domain (PH<sup>FAPP1</sup>) and accumulates in epidermal root cells (Vermeer et al., 2009; Simon et al., 2014). YFP fluorescence in the cytoplasm is indicative of a free biosensor, whereas YFP signals at the membrane can be used as an indirect measure of PI4P abundance in a particular compartment.

PI4P is primarily enriched at the plasma membrane and is also localized to intracellular compartments, such as TGN/EE (Simon et al., 2014). As expected, under normal growth conditions, PI4P was primarily detected at the cell periphery and was also visible as dotted intracellular structures (Fig. 4A; Supplemental Fig. S2A). PI4P levels were monitored in the subcellular compartments over the course of 120 min (Fig. 4, C and D; Supplemental Fig. S2A). PI4P levels at the plasma membrane increased after 60 min, most likely in response to the DMSO present in the culture medium, whereas the levels of the biosensor decreased in the intracellular compartments at 120 min (Fig. 4, C and D).

Upon Sortin2 treatment, PI4P retained its two subcellular localizations, but its dynamics changed compared with the control (Fig. 4, C and D; Supplemental Fig. S2A). Exposure to Sortin2 induced a transient increase in PI4P levels at the plasma membrane after 30 min compared with the control (Fig. 4C). Subsequently, PI4P levels at the plasma membrane gradually decreased at 60 and 90 min, recovering to levels similar to those observed at the beginning of the experiment after 120 min of incubation (Fig. 4C; Supplemental Fig. S2A). Sortin2 induced a transient increase in the endosome pool of PI4P compared with the control (Fig. 4, A and D; Supplemental Fig. S2A).

We also detected a gradual increase in intracellular-labeled structures at 30 to 90 min of Sortin2 treatment, followed by a drop at 120 min to control levels (Fig. 4, A

and D; Supplemental Fig. S2A). This transient increase in intracellular PI4P levels was not due to a net increase in YFP fluorescence in response to Sortin2 treatment (Supplemental Fig. S2C). Therefore, Sortin2 treatment induced two types of changes in PI4P levels: (1) PI4P levels increased, followed by a decrease, at the plasma membrane; and (2) PI4P levels increased at the endosomal compartment. These effects lasted less than 120 min, after which point PI4P levels in both compartments became similar to those of the control.

The localization of PI4P was not affected by 0.1  $\mu\text{M}$  PAO treatment (Fig. 4B; Supplemental Fig. S2B), suggesting that PI4K activity is not completely abolished by this submicromolar concentration of PAO. However, the increase in PI4P levels at the plasma membrane under control conditions was impaired by 0.1  $\mu\text{M}$  PAO treatment (Fig. 4E), suggesting that some of the activity of PI4K is sensitive to this concentration of PAO. Moreover, the effect of Sortin2 on PI4P levels in both compartments was abolished by 0.1  $\mu\text{M}$  PAO treatment (Fig. 4, B, E, and F; Supplemental Fig. S2B), highlighting the key role played by PI4K in regulating PI4P levels in response to Sortin2, specifically PI4K activity that is sensitive to this submicromolar concentration of PAO.

Treatment with 20  $\mu\text{M}$  PAO blocked localization of the PI4P biosensor to the intracellular compartments, resulting in its cytoplasmic distribution (Supplemental Fig. S2E). This result indicates that a drastic drop in PI4P levels occurred, which is consistent with previous reports (Vermeer et al., 2009; Simon et al., 2016). Under this condition, endocytic trafficking was blocked (Supplemental Fig. S1) and eLR formation was impaired (Fig. 1B). These results suggest that PI4P functions in LR formation either via a developmentally controlled mechanism or via a mechanism triggered by Sortin2 or NAA treatment. Sortin2 failed to overcome the abolition of PI4K activity, indicating that PI4P is required for LRP formation (Fig. 1) and for Sortin2-induced endocytic trafficking (Fig. 2). We conclude that Sortin2 increases PI4P levels due to PI4K activity, which is crucial for Sortin2-induced LRP formation. Therefore, variation in PI4P abundance due to PI4K activity is a key molecular component in endocytic trafficking-dependent LRP formation.

### PI4KIII $\beta$ 1 and PI4KIII $\beta$ 2 Are Key Modulators of LRP Formation Driven by Endocytic Trafficking to the Vacuole

The enzymatic activities of PI4KIII $\beta$ 1 and PI4KIII $\beta$ 2 have been confirmed (Mueller-Roeber and Pical, 2002; Delage et al., 2012); the loss-of-function of both of these proteins in the *pi4kiii $\beta$ 1 pi4kiii $\beta$ 2* double mutant results in defects in root hair polarity and primary root length (Preuss et al., 2006). Due to the involvement of PI4K in LRP formation caused by accelerated endocytic trafficking, we analyzed the effect of Sortin2 on *pi4kiii $\beta$ 1 pi4kiii $\beta$ 2*. Sortin2 failed to stimulate LRP formation in *pi4kiii $\beta$ 1 pi4kiii $\beta$ 2* (Fig. 5A, black bars). However, this

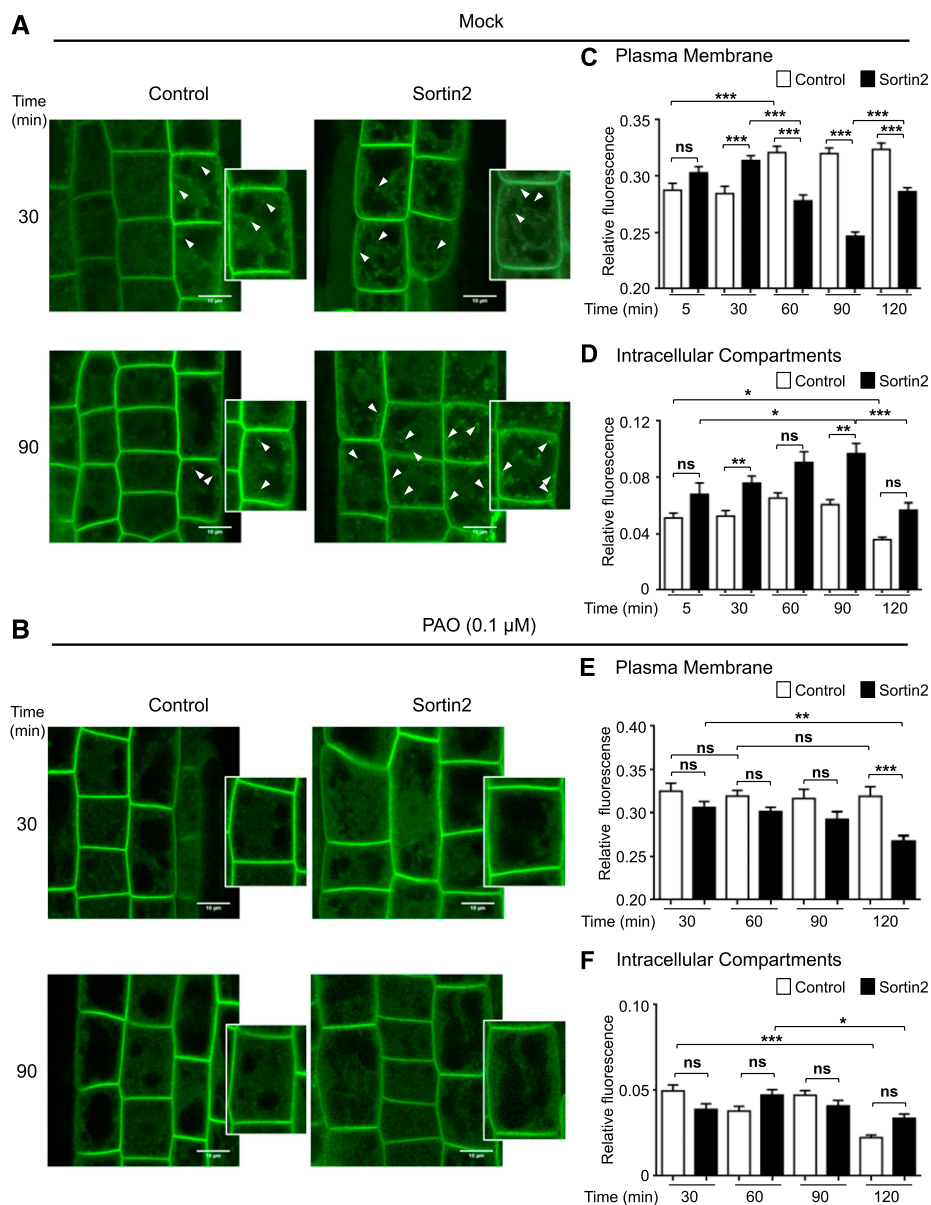


**Figure 4.** Chemical stimulation of endocytic trafficking induces changes in PI4P levels, which are dependent on PI4K activity. Evaluation of PI4P levels in 7-d-old YFP-PH<sup>FAPP1</sup> transgenic seedlings was completed. Seedlings were preincubated in MSL with 0.1  $\mu$ M PAO for 60 min (B). Mock treatment (without PAO) was used for comparison (A). The seedlings were subsequently incubated in 58  $\mu$ M Sortin2 or under control conditions and recruitment of the sensor was evaluated. PAO levels were maintained at 0.1  $\mu$ M throughout the Sortin2 treatment. A and B, Representative confocal single images showing PI4P biosensor signals in epidermal root cells after 30 and 90 min of treatment. An individual cell in an image with higher magnification and brightness is shown for each condition. Arrowheads indicate intracellular compartments. Scale bars = 10  $\mu$ m. C to F, Evaluation of the recruitment of the PI4P biosensor to the plasma membrane and endosomes under mock treatments (C and D) and treatment with 0.1  $\mu$ M PAO (E and F). Fluorescence intensity at the plasma membrane (C and E) and intracellular compartments (D and F) was quantified and normalized to the fluorescence of the whole cell. White and black bars represent control and Sortin2 treatment, respectively. Epidermal root cells from different seedlings were evaluated in experimental triplicates (C and D,  $n = 58$ –93 control from 7–10 roots, 58–132 Sortin2 from 4–10 roots; E and F,  $n = 58$ –75 control from 7–12 roots, 62–79 Sortin2 from 9–15 roots). Two-way ANOVA with Sidak's multiple comparisons test was performed (C, E, and F). In D, a Kruskal-Wallis test with Dunn's multiple comparisons test was performed because the data did not fit a Gaussian distribution. \*\*\* $P < 0.001$ ; \*\* $P < 0.01$ ; \* $P < 0.05$ ; not significant (ns):  $P > 0.05$ . Error bars denote SEM.

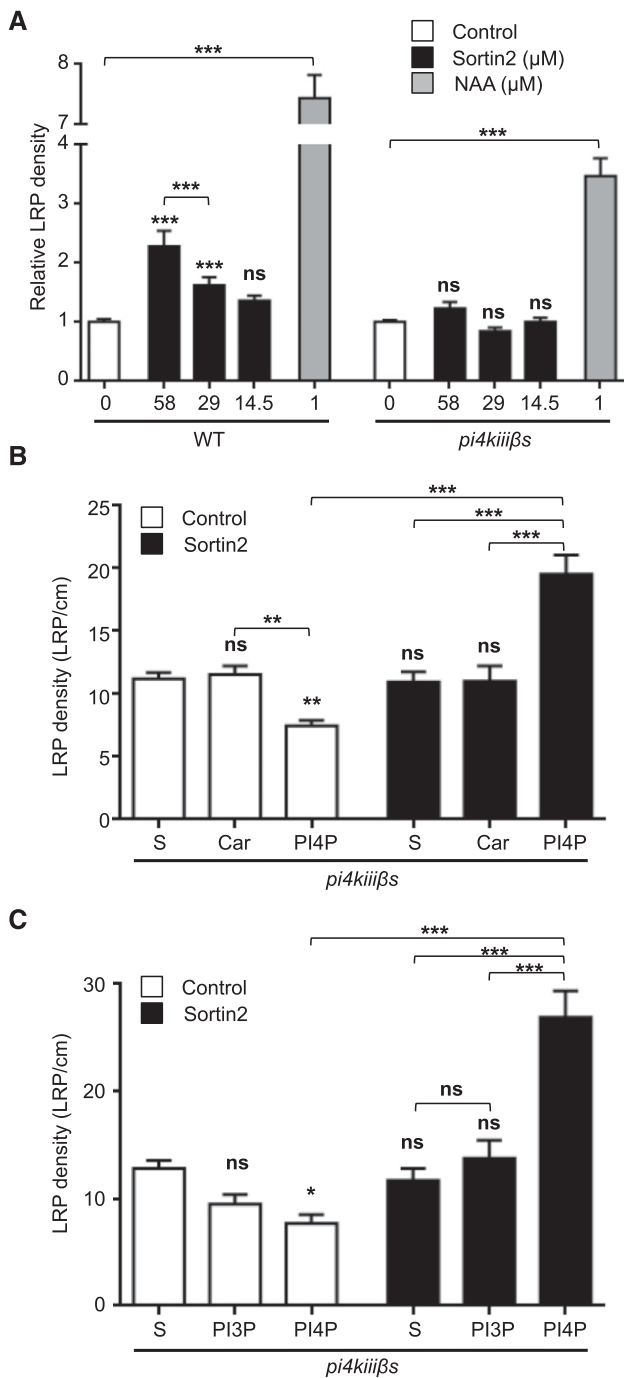


**Figure 5.** PI4KIIIβ1 and PI4KIIIβ2 activity is essential for Sortin2-induced LRP formation. **A**, Col-0 [7 d old; wild type (WT)] and *pi4kiiiβ1 pi4kiiiβ2* (*pi4kiiiβs*) seedlings were treated with MSL containing 58, 29, or 14.5 μM Sortin2 (black bars), 1 μM NAA (gray bar), and control conditions (1% [v/v] DMSO, white bar). After 3 D, LRP density was scored relative to control conditions for each genetic background ( $n = 29$  wild type and 44 *pi4kiiiβs* seedlings in control, 16 to 17 wild type and 21–32 *pi4kiiiβs* seedlings in Sortin2, 14 wild type and 20 *pi4kiiiβs* seedlings in NAA). **B**, Exogenous PI4P was added to 5-d-old *pi4kiiiβs* seedlings to evaluate the rescue of the mutant phenotype. PI4P was added at a ratio of 15 μM:15 μM PI4P:Carrier3 complex (PI4P). Seedlings incubated in organic solvent (S) or Carrier3 (Car) alone were

mutant retained the capacity to develop more LRPs in response to an exogenous stimulus, such as the auxin NAA (Fig. 5A, gray bar). These results indicate that loss of function of *PI4KIIIβ1* and *PI4KIIIβ2* specifically disrupts the mechanism induced by Sortin2. Therefore, both *PI4KIIIβ1* and *PI4KIIIβ2* are essential for LRP formation driven by the induction of endocytic trafficking.

The *pi4kiiiβ1 pi4kiiiβ2* mutant has lower levels of PI4P than wild-type seedlings, consistent with its reduced PI4K activity (Delage et al., 2012). Therefore, the inability of *pi4kiiiβ1 pi4kiiiβ2* to develop Sortin2-induced LRP is most likely due to its reduced PI4P levels. To investigate this possibility, we compensated for the reduced levels of PI4P in *pi4kiiiβ1 pi4kiiiβ2* via exogenous treatment with PI4P. This treatment is effective in Arabidopsis (Zheng et al., 2014). Indeed, the addition of PI4P, along with a carrier protein, rescued the defective primary root phenotype of the double mutant, suggesting that exogenous application of PI4P was effective for increasing PI4P levels, at least in root tissue (Supplemental Fig. S3C). Indeed, exogenous supplementation with PI4P restored the association of the PI4P biosensor with the plasma membrane, which was impaired by the 20 μM PAO treatment in root cells (Supplemental Fig. S2F). Furthermore, *pi4kiiiβ1 pi4kiiiβ2* developed more LRPs in response to Sortin2 when exogenous PI4P was supplied (Fig. 5B). By contrast, exogenous PI3P had no effect on the sensitivity of the double mutant to Sortin2-induced LRP formation (Fig. 5C).

These results confirm that this inability of *pi4kiiiβ1 pi4kiiiβ2* to develop LRPs in response to Sortin2 is due to its defect in PI4P levels. Therefore, the formation of the enzymatic product of PI4K (PI4P) is required for LRP formation induced by Sortin2. This conclusion is consistent with the finding that PI4P levels increase after Sortin2 stimulation and that PI4P is required to induce LRP formation (Figs. 1 and 4). Furthermore, the PI4P levels required for this developmental process are specifically dependent on the enzymatic activities of *PI4KIIIβ1* and *PI4KIIIβ2* in Arabidopsis.

Due to the essential roles of *PI4KIIIβ1* and *PI4KIIIβ2* in Sortin2-induced LRP formation, we next evaluated their roles in endocytic trafficking to the vacuole.

used as controls to probe the specific effect of PI4P. LRP density was evaluated in seedlings after 5 d of treatment with 58 μM Sortin2 (black bars) or under control conditions (1% [v/v] DMSO; white bar) in two independent experiments ( $n = 19–25$  seedlings in control, 14–16 seedlings in Sortin2). **C**, A similar experiment to (B) was performed to test the effect of exogenous PI3P [added at a ratio of 15 μM:15 μM PI3P:Carrier3 complex (PI3P)]. In addition, exogenous PI4P treatment was run in parallel to compare the effects of both lipids. Three independent experiments were performed ( $n = 20$  control seedlings and 8–12 Sortin2-treated seedlings, for each experimental condition). One-way (A) and two-way (B and C) ANOVA with Sidak's multiple comparisons test were performed. \*\*\* $P < 0.001$ ; \*\* $P < 0.01$ ; \* $P < 0.05$ ; not significant (ns):  $P > 0.05$  compared with the corresponding control (symbol above each bar) or between conditions. Error bars denote SEM.



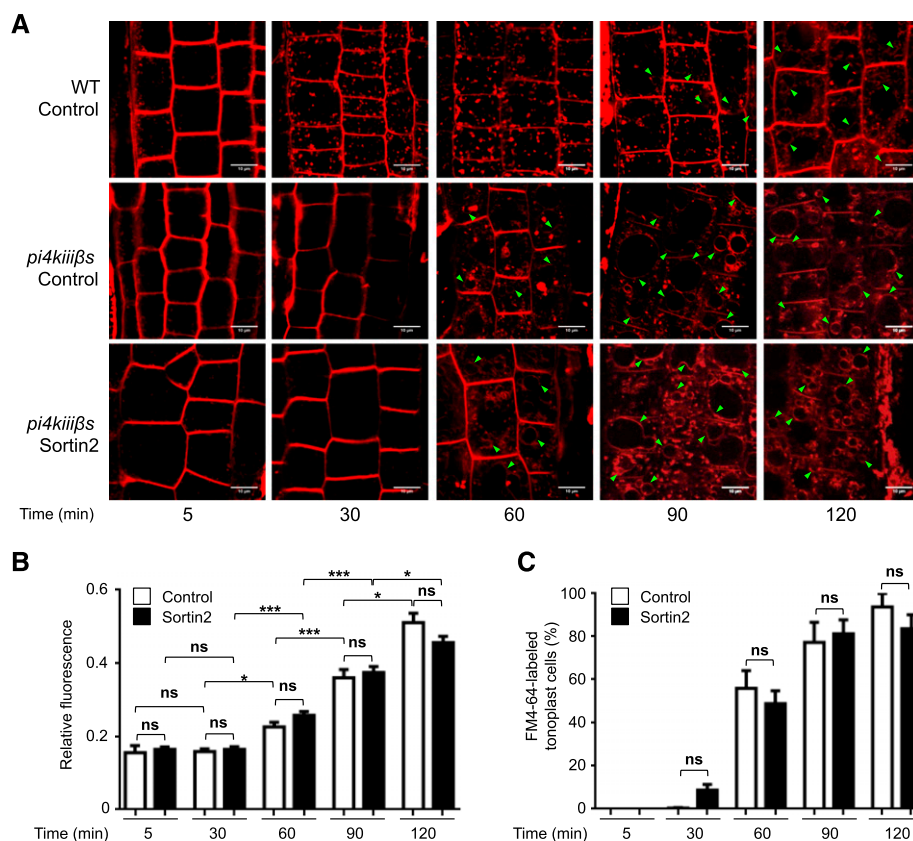


**Figure 6.** The loss of function of *PI4KIII $\beta$ 1* and *PI4KIII $\beta$ 2* results in a higher rate of endocytic trafficking to the vacuole, which is not affected by Sortin2. **A**, FM4-64 endocytic kinetics in epidermal root cells in 7-d-old Col-0 [wild type (WT) control] and *pi4kiii $\beta$ 1 pi4kiii $\beta$ 2* (*pi4kiii $\beta$ s* control) seedlings under control conditions. FM4-64 endocytic kinetics of 7-d-old *pi4kiii $\beta$ 1 pi4kiii $\beta$ 2* seedlings was also evaluated in the presence of 58  $\mu$ M Sortin2 (*pi4kiii $\beta$ s* Sortin2). Representative single confocal images of FM4-64 internalization in experimental triplicates in different time periods are shown. Arrowheads indicate FM4-64-stained tonoplasts. Scale bars = 10  $\mu$ m. **B**, Quantification of FM4-64 internalized in subcellular compartments in *pi4kiii $\beta$ 1 pi4kiii $\beta$ 2* epidermal root cells shown in (A). FM4-64 fluorescence was normalized to the fluorescence of the whole cell. **C**, The number of epidermal root cells with stained tonoplast under the conditions described in (A) was quantified and expressed as the percentage of the evaluated cells. **B** and **C** correspond to  $n = 48$ –130 root cells from 8–13 control seedlings and 120–203 cells from 13–23 Sortin2-treated seedlings. Two-way ANOVA with Sidak's multiple comparisons test was performed. \*\*\* $P < 0.001$ ; \*\* $P < 0.01$ ; \* $P < 0.05$ ; not significant (ns):  $P > 0.05$ . Error bars denote SEM.

Specifically, we analyzed FM4-64 internalization in *pi4kiii $\beta$ 1 pi4kiii $\beta$ 2* over time. The double mutant displayed larger FM4-64-stained endosomes than wild-type seedlings (Fig. 6A, 60 min), which is consistent with the altered trans-Golgi network structure resulting from the loss of function of *PI4KIII $\beta$ 1* and *PI4KIII $\beta$ 2* (Kang et al., 2011). When compared with the wild type, fewer FM4-64-stained endosomes were observed at 5 and 30 min in the double mutant (Fig. 6A). By contrast, endocytic trafficking to the vacuole was accelerated in *pi4kiii $\beta$ 1 pi4kiii $\beta$ 2*, as FM4-64 reached the vacuole in a shorter time (within 60 min) in the double mutant than in wild-type seedlings (within 90 min; Fig. 6A).

FM4-64 trafficking from the plasma membrane to endosomes was inhibited in the double mutant, which is consistent with the impaired FM4-64 internalization recently described by Lin et al. (2019). However, the tracer reached the vacuole more rapidly in the double

mutant than in the wild type. This finding suggests that trafficking to the vacuole is highly stimulated in *pi4kiii $\beta$ 1 pi4kiii $\beta$ 2* to compensate for the initial inhibition of plasma membrane-to-endosome trafficking. The loss of function of *PI4KIII $\beta$ 1* and *PI4KIII $\beta$ 2* appears to mimic the response of wild-type seedlings to Sortin2. Therefore, *PI4KIII $\beta$ 1* and *PI4KIII $\beta$ 2* are required for the internalization of the plasma membrane that underlies endosome formation. Furthermore, these enzymes negatively regulate trafficking to the vacuole. Sortin2 failed to induce the internalization of FM4-64 from the plasma membrane to endosomes in *pi4kiii $\beta$ 1 pi4kiii $\beta$ 2* seedlings (Fig. 6, A and B). Moreover, Sortin2 failed to further increase the rate of trafficking to the vacuole in the double mutant (Fig. 6, A and C).

These observations are consistent with the finding that Sortin2 did not induce LRP formation in *pi4kiii $\beta$ 1 pi4kiii $\beta$ 2* (Fig. 5A). These results confirm the requirement



of *PI4KIIIβ1* and *PI4KIIIβ2* for LRP formation promoted by the acceleration of endocytic trafficking to the vacuole in response to Sortin2.

#### Chronic Inhibition of PI4K Activity Induces Endocytic Trafficking to the Vacuole, thereby Affecting LRP Formation

We noticed that treatment with PI4P affected LRP formation in *pi4kiiiβ1 pi4kiiiβ2* (Fig. 5B). Indeed, the number of LRPs decreased by 33% in the double mutant supplemented with PI4P (Fig. 5B) without apparently affecting eLR formation (Supplemental Fig. S3C). The addition of PI3P to *pi4kiiiβ1 pi4kiiiβ2* did not produce any changes in LRP formation in the presence or absence of Sortin2, indicating that PI4P plays a specific role in this process (Fig. 5C). Therefore, the lower levels of PI4P caused by the loss of function of *PI4KIIIβ1* and *PI4KIIIβ2* resulted in a higher number of LRPs in the double mutant. This contradicts the notion that PI4P is required for Sortin2-driven LRP formation.

We investigated whether *pi4kiiiβ1 pi4kiiiβ2* displayed an LR phenotype by analyzing the root system architecture of 10-d-old double mutant seedlings. Indeed, under normal conditions, *pi4kiiiβ1 pi4kiiiβ2* seedlings displayed an increased number of LRPs compared with the wild type (Fig. 7, B and C, respectively). Seedlings (10 d old) displayed a 110% increase in LRP formation, which was sustained as the plants aged (Fig. 7B).

In the primary root, LRPs are generated in the FZ, and after development, they emerge in the BZ (Dubrovsky and Forde, 2012). In wild-type Arabidopsis, the FZ is shorter than the BZ (Fig. 7A). However, *pi4kiiiβ1 pi4kiiiβ2* displayed a relatively long FZ in proportion to the BZ (Fig. 7A). Furthermore, we observed an increase in LRP formation in both the FZ and BZ of *pi4kiiiβ1 pi4kiiiβ2*, confirming that the LRP formation mechanism is highly induced in this mutant (Fig. 7B). This increase was maintained in 14-d-old plants (Fig. 7B). The increase in eLR formation in *pi4kiiiβ1 pi4kiiiβ2* became evident only in 14-d-old plants, which could be explained by the increase in LRP formation observed during the earlier stages (Fig. 7C). This mutant phenotype suggests that *PI4KIIIβ1* and *PI4KIIIβ2* play negative roles in LRP formation (Fig. 7B). The LRP overproduction in *pi4kiiiβ1 pi4kiiiβ2* indicates that *PI4KIIIβ1* and *PI4KIIIβ2* are negative regulators of LRP formation. However, in wild-type seedlings, interfering with PI4K activity by a 3-d treatment with 0.1  $\mu\text{M}$  PAO did not alter LRP formation (Fig. 1A) or endocytic trafficking to the vacuole (Fig. 2B). Perhaps the genetic loss of function of the *PI4KIIIβs* activates a compensatory mechanism for LRP formation that depends on endocytic trafficking to the vacuole, which is also stimulated in the double mutant, as mentioned above.

The genetic loss of function of PI4K could be mimicked by the chronic chemical inhibition of its enzymatic activity. Therefore, we investigated the effect of

applying PAO before seed germination to chemically provoke the loss of function of PI4K activity. Indeed, wild-type seedlings grown in the presence of 0.1  $\mu\text{M}$  PAO since seed sowing displayed a defect in root hair polarity resembling the *pi4kiiiβ1 pi4kiiiβ2* phenotype described by Preuss et al. (2006; Supplemental Fig. S4A). Furthermore, the chemically induced loss of function of PI4K induced vacuole fragmentation comparable with that of *pi4kiiiβ1 pi4kiiiβ2* (Supplemental Fig. S4B).

Because chronic chemical inhibition proved to be effective, we evaluated its impact on root system architecture and endocytic trafficking (Fig. 8). When wild-type seedlings were grown in 0.1 or 1  $\mu\text{M}$  PAO, LRP formation increased (Fig. 8A), whereas the number of eLRs was not altered by a 0.1 or 1  $\mu\text{M}$  PAO treatment (Fig. 8B). Therefore, the addition of PAO from germination to the seedling stage mimicked the phenotype of the genetic loss of function of *PI4KIIIβ1* and *PI4KIIIβ2*. By contrast, 0.1 and 1  $\mu\text{M}$  PAO treatment had no effect on LRP formation in the *pi4kiiiβ1 pi4kiiiβ2* mutant (Fig. 8A). The insensitivity of the *pi4kiiiβ1 pi4kiiiβ2* mutant to PAO supports the notion that the targets of low doses of PAO are *PI4KIIIβ1* and *PI4KIIIβ2*. Moreover, this result confirms that these two proteins are crucial for LRP formation. The doses of PAO that completely inhibited endocytosis from the plasma membrane, even in *pi4kiiiβ1 pi4kiiiβ2* (20  $\mu\text{M}$  and 10  $\mu\text{M}$ ; Supplemental Fig. S5), did not promote LRP formation in wild-type or *pi4kiiiβ1 pi4kiiiβ2* plants (Fig. 8A). Indeed, 20  $\mu\text{M}$  PAO inhibited LRP formation in the *pi4kiiiβ1 pi4kiiiβ2* mutant to levels similar to those observed in the wild type (Fig. 8A). Therefore, PI4K enzymes other than *PI4KIIIβ1* and *PI4KIIIβ2* are also important for LR organogenesis.

Chronic PI4K inhibition by 0.1  $\mu\text{M}$  PAO in wild-type seedlings induced endocytic trafficking to the vacuole, as FM4-64 reached the tonoplast at an earlier time point (60 min) in a higher proportion of epidermal root cells compared with the control, i.e. 58.9% of cells in PAO-sown seedling compared with 27.6% in the control (Fig. 8C). Consistently, under this condition, FM4-64-stained endosomes were enlarged, as were *pi4kiiiβ1 pi4kiiiβ2* endosomes (compare Fig. 6A to Fig. 8C, at 60 min). Therefore, plants exposed to chronic chemical inhibition of PI4K activity exhibited an endocytic trafficking phenotype similar to that of the *PI4KIIIβ1* and *PI4KIIIβ2* genetic loss-of-function mutant. However, the inhibition of *PI4KIIIβ1* and *PI4KIIIβ2* activity by a 3-d treatment with 0.1  $\mu\text{M}$  PAO did not alter the timing of trafficking from the plasma membrane to the vacuole (Fig. 2B). These contrasting effects strengthen the idea that a compensatory mechanism takes place when the functions of both *PI4KIIIβ1* and *PI4KIIIβ2* are chronically inhibited, leading to the induction of endocytic trafficking and LRP formation. Overall, these results confirm that *PI4KIIIβ1* and *PI4KIIIβ2* are indeed the PI4Ks that participate in LRP formation driven by endocytic trafficking.

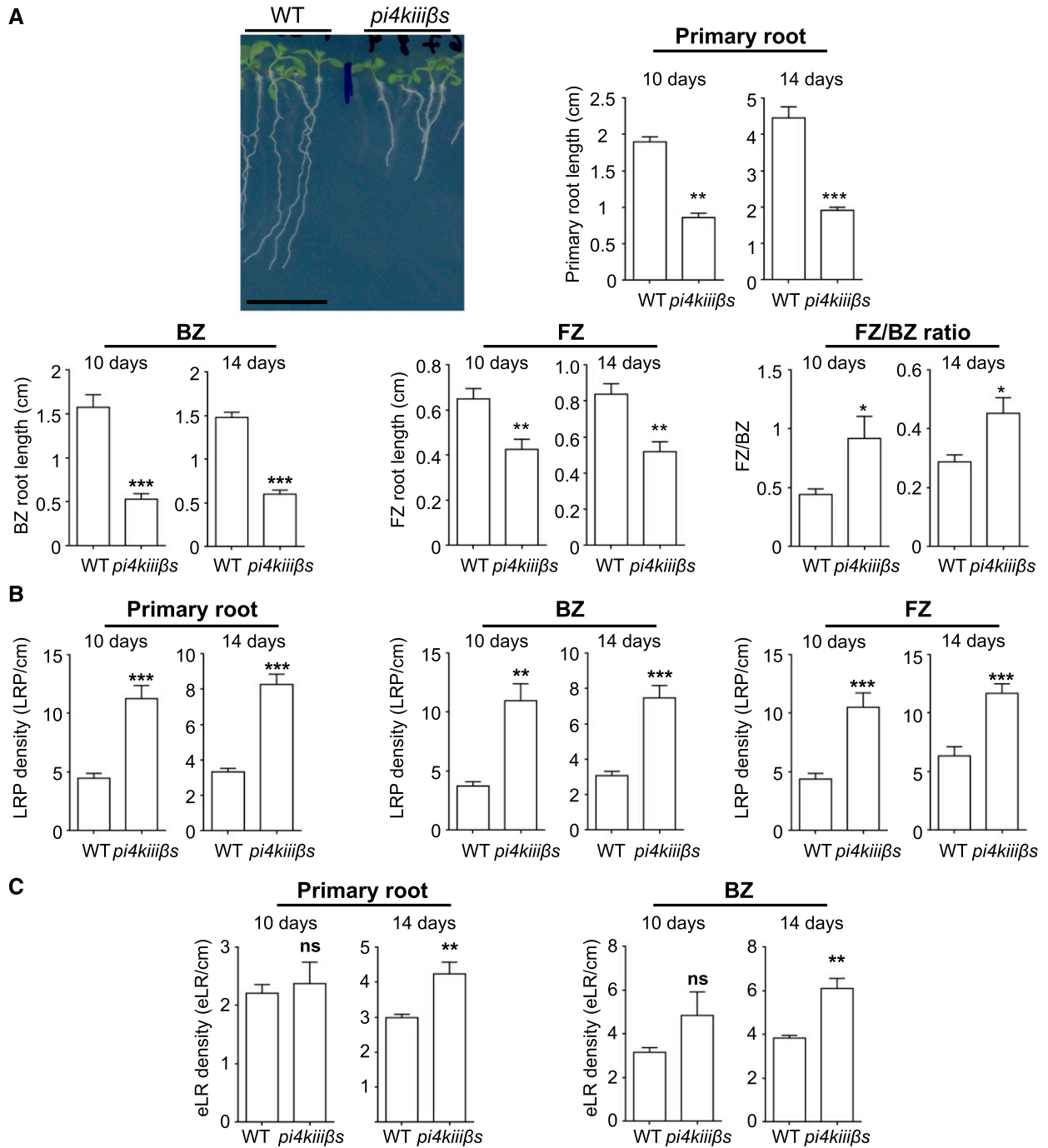


**Figure 7.** The loss of function of *PI4KIIIβ1* and *PI4KIIIβ2* promotes root branching. A, Col-0 [10 d old; wild type (WT)] and *pi4kiiiβ1 pi4kiiiβ2* loss-of-function mutant (*pi4kiiiβs*) seedlings are shown. Scale bar = 1 cm. The length of the primary root was measured in 10- and 14-d-old seedlings. The length of the branching zone (BZ) and formation zone (FZ) of Col-0 and *pi4kiiiβs* primary roots was evaluated in 10- and 14-d-old seedlings. The ratio of FZ/BZ length is also shown. The primary root zones were defined according to Dubrovsky and Forde (2012). B, LRP density in 10- and 14-d-old Col-0 (wild type) and *pi4kiiiβs* seedlings ( $n = 11$  wild type and 9 *pi4kiiiβs* seedlings). LRP density values in the entire primary root, BZ, and FZ are shown. C, The density of eLRs in the entire primary root and its BZ in 10- and 14-d-old Col-0 (wild type) and *pi4kiiiβs* seedlings. A to C, Results from three independent experiments are shown ( $n = 11$  wild type and 9 *pi4kiiiβs* seedlings). Two-tailed Student's *t* test was performed: \*\*\* $P < 0.001$ ; \*\* $P < 0.01$ ; \* $P < 0.05$ . Error bars denote SEM.

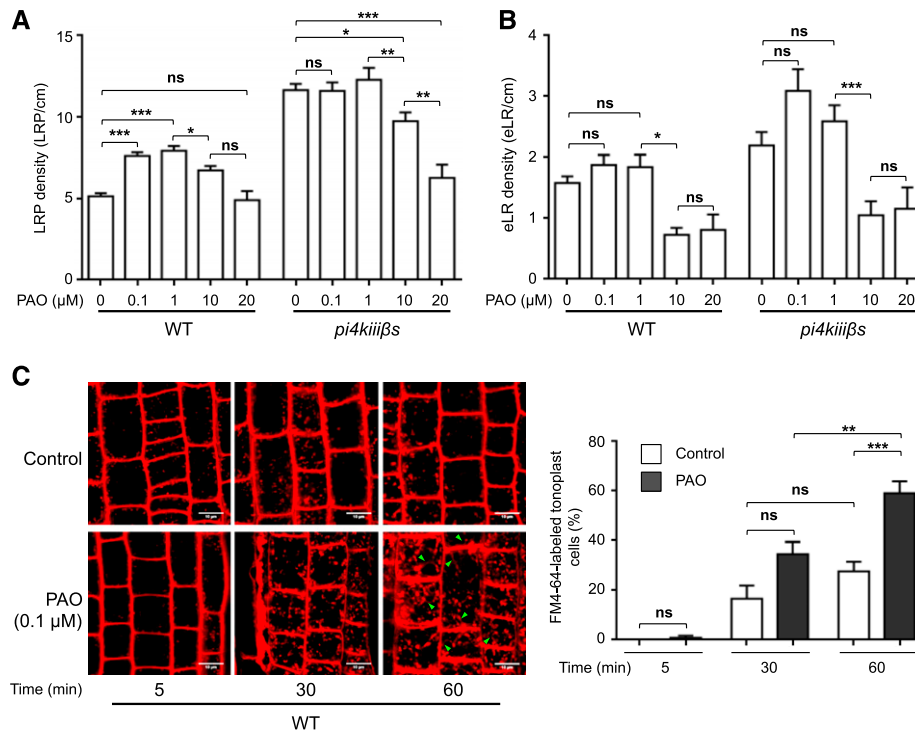


**Figure 8.** Chronic inhibition of PI4K activity positively affects endocytic trafficking to the vacuole and stimulates LRP formation. A and B, The effect of chronic treatment with PAO on Col-0 [wild type (WT)] and *pi4kiiiβ1 pi4kiiiβ2*. Seeds were incubated for 10 d in MSS containing 0.1, 1, 10, or 20 μM PAO. Incubation with MSS supplemented with 1% (v/v) DMSO was used as the control (0 μM PAO). LRP (A) and eLR (B) density was evaluated ( $n = 20\text{--}37$  wild type and 16–40 *pi4kiiiβs* seedlings per condition). Two-way ANOVA with Sidak’s multiple comparisons test was performed. \*\*\* $P < 0.001$ ; \*\* $P < 0.01$ ; \* $P < 0.05$ ; ns (not significant):  $P > 0.05$ . Error bars denote SEM. C, Endocytic trafficking of FM4-64 evaluated in 7-d-old Col-0 (wild type) seedlings treated with 0.1 μM PAO or 1% (v/v) DMSO (control) beginning at germination. PAO or DMSO levels were maintained throughout the FM4-64 internalization assay. Representative confocal images of FM4-64 internalization in experimental triplicates at different time points are shown. Arrowheads indicate FM4-64-stained tonoplast. Scale bar = 10 μm. Epidermal root cells with stained tonoplast were quantified and expressed as a percentage of the evaluated cells ( $n = 84\text{--}329$  cells from 6–15 seedlings in control and 94–410 cells from 6–20 seedlings in the PAO condition). Two-way ANOVA with Sidak’s multiple comparisons test was performed. \*\*\* $P < 0.001$ ; \*\* $P < 0.01$ ; \* $P < 0.05$ ; not significant (ns):  $P > 0.05$ . Error bars denote SEM.

## DISCUSSION

In this study, we evaluated the role of PI4K activity in endocytic trafficking–dependent LR organogenesis via chemical stimulation with Sortin2. This chemical stimulation induced changes in PI4P levels in subcellular compartments in conjunction with the induction of an endocytic pathway to the vacuole, leading to LRP formation. The increase in PI4P levels in response to Sortin2 stimulation is mediated by the PI4Ks PI4KIIIβ1 and PI4KIIIβ2. By contrast, chronic chemical and genetic inhibition of both enzymes had a positive effect on LRP formation due to the induction of trafficking to the vacuole. Therefore, PI4KIIIβ1 and PI4KIIIβ2 negatively regulate developmentally controlled LR organogenesis in wild-type Arabidopsis.

### The Role of PI4K in LRP Formation Induced by Endocytic Trafficking

The requirement of PI4K activity for the mode of action of Sortin2 suggests that PI4KIIIβ1 and PI4KIIIβ2

are the cognate targets of this bioactive chemical. The insensitivity displayed by the double mutant *pi4kiiiβ1 pi4kiiiβ2* (Fig. 5A) reinforced this idea. However, the ability to develop LRPs in response to Sortin2 was restored by the addition of exogenous PI4P. Under such conditions, Sortin2 was able to exert its role in LRP formation even in the absence of PI4KIIIβs (Fig. 5B). Therefore, during root organogenesis, the cognate target(s) of Sortin2 is likely a molecular component upstream of the PI4KIIIβs. Indeed, the effect of Sortin2 on endocytosis from the plasma membrane was observed after only 5 min (Fig. 2A; Pérez-Henríquez et al., 2012), whereas an increase in PI4P levels was detected after 30 min (Fig. 4, C and D), suggesting that endocytosis from the plasma membrane is the leading cellular event in this process.

PI4P is present at the plasma membrane and the FM4-64-labeled intracellular compartment identified as the TGN/EE membranes (Vermeer et al., 2009; Simon et al., 2014, 2016; Tejos et al., 2014). Treatment with Sortin2 promoted changes in PI4P levels in the

membranes, where this lipid is normally synthesized (Fig. 4). After chemical stimulus, PI4P levels increased at the plasma membrane before increasing at the endocytic downstream compartment TGN/EE, suggesting the presence of a cascade event (Fig. 4). A sub-micromolar dose of PAO (0.1  $\mu$ M) drastically repressed LRP formation, specifically in response to these changes in PI4P enrichment in the membrane (Fig. 1A). This concentration of PAO particularly targets PI4KIII $\beta$ s proteins, as revealed by the insensitivity of *pi4kiii $\beta$ 1 pi4kiii $\beta$ 2* to 0.1 and 1  $\mu$ M PAO (Fig. 8A). Therefore, these PI4Ks are essential for increasing PI4P levels induced by Sortin2 (Fig. 4) and for LRP formation in response to the induction of endocytic trafficking (Figs. 1–3).

PI4KIII $\beta$ 1 is most likely responsible for raising PI4P levels at the TGN/EE, the subcellular location in which this protein is enriched (Preuss et al., 2006; Kang et al., 2011; Lin et al., 2019). Because PI4KIII $\beta$ 1 has not been detected at the plasma membrane, the increase in PI4P levels at the plasma membrane is likely due to PI4KIII $\beta$ 2 activity. Although the membrane localization of PI4KIII $\beta$ 2 has not been reported, platforms such as Bio-Analytic Resource have identified interactions of PI4KIII $\beta$ 2 with several plasma membrane-localized proteins, which is consistent with the observation that PI4KIII $\beta$ 2-GFP fusion protein accumulates at the plasma membrane in Arabidopsis roots (Okazaki et al., 2015).

After PI4P levels increased in response to Sortin2, PI4P levels dropped at the plasma membrane as well as the TGN/EE (Fig. 4, C and D), which is consistent with the dynamic metabolism of phosphoinositides (PIs). After their biosynthesis, PIs are rapidly used as substrates by kinases, phosphatases, and lipases (Boss and Im, 2012; Heilmann, 2016). PI4P could be phosphorylated by the PI4P 5-kinase (PI4P5K), generating PI(4,5)P<sub>2</sub> (Munnik and Nielsen, 2011; Heilmann, 2016). PI4P5K activity and PI(4,5)P<sub>2</sub> levels increase at the plasma membrane and intracellular membranes in response to various stimuli (Im et al., 2007; van Leeuwen et al., 2007; Mishkind et al., 2009), which is accompanied by a decrease in PI4P levels (König et al., 2008). Subsequently, PI4P5K activity could be responsible for the decrease in PI4P levels detected after chemical stimulation (Fig. 4). Whether the metabolism of PI4P is part of the signaling pathway for LRP formation, the progression of endocytosis, or simply a mechanism used to reestablish PI4P levels, is unknown.

#### PI4KIII $\beta$ -Dependent Endocytic Trafficking and its Impact on LR Organogenesis

The increase in PI4P levels induces the recruitment of PI4P-interacting proteins to enable or initiate the cascade of downstream events. RAB proteins are small GTPases that regulate membrane trafficking, as their activated forms bind to specific endomembrane compartments and recruit other proteins. PI4KIII $\beta$ 1 and

RABA4b are localized to the TGN/EE (Kang et al., 2011), strongly suggesting this complex plays a role in vesicle trafficking. Notably, PI4K of the  $\alpha$  and  $\gamma$  families of Arabidopsis is unable to interact with RAB4Bb (Preuss et al., 2006). Because the loss of function of the PI4KIII $\beta$ s is sufficient for abolishing the response to Sortin2, the PI4KIII $\beta$ s/RABA4b complex most likely mediates membrane trafficking leading to LRP formation.

Furthermore, PI4P recruits proteins containing lipid binding domains (Heilmann, 2016), such as the ubiquitin E3 ligase PLANT U-BOX13 (PUB13; Mudgil et al., 2004). Indeed, the interaction among RABA4b, PUB13, and PI4KIII $\beta$ 1, along with other PI4P interactors, constitutes a TGN microdomain that participates in redirecting proteins from the plasma membrane toward late endosomes/prevacuolar compartments (Antignani et al., 2015). Therefore, the TGN PI4KIII $\beta$  microdomain might participate in endocytic protein relocation leading to LR organogenesis. Although PUB13 is associated with PI4KIII $\beta$ s in leaves, their physical association in root tissues has not been analyzed. Sortin2-induced endocytic trafficking of FM4-64 to the vacuole was impaired by the chemical inhibition of PI4KIII $\beta$  activity (Figs. 2 and 3). However, the induction of endocytosis was not abolished by this treatment (Fig. 2). Because FM4-64 traces all trafficking routes to the vacuole, PI4KIII $\beta$ s activities likely play a role in at least one of the three routes for delivering cargo from the TGN/EE to the vacuole described in Arabidopsis (Ebine et al., 2014). Such a route and/or cargo is crucial for LR organogenesis, since its interference abolishes LRP formation (Fig. 1).

#### The Dual Role of PI4KIII $\beta$ s in LRP Formation

Surprisingly, both the chronic chemical inhibition and genetic loss of function of PI4KIII $\beta$ s resulted in increases in both LRP formation and endocytic trafficking to the vacuole (Figs. 6, 7, and 8). Therefore, it appears that PI4KIII $\beta$ 1 and PI4KIII $\beta$ 2 constitutively inhibit the LR organogenesis induced by a pathway that depends on endocytic trafficking. PI4Ks function as negative regulators in various physiological processes in response to external stimuli (Šašek et al., 2014; Okazaki et al., 2015). The chemical stimulus of Sortin2 increases PI4K activity and PI4P levels as well as LRP formation. By contrast, LRP formation is promoted even though the loss of function of *PI4KIII $\beta$ 1* and *PI4KIII $\beta$ 2* causes a decrease in PI4P levels (Delage et al., 2012). Indeed, exogenous PI4P treatment, but not PI3P treatment, rescued the LRP phenotype of the *pi4kiii $\beta$ 1 pi4kiii $\beta$ 2* mutant. These observations suggest that PI4P is a key dual regulator of LRP formation, functioning as a negative regulator of developmentally controlled LRP formation and a positive regulator of LRP formation induced by Sortin2 exposure.

We propose that under normal conditions, basal levels of PI4P recruit proteins with a high affinity for PI4P that negatively regulate endocytic trafficking and



LRP formation. In the chronic absence of PI4KIII $\beta$  function, PI4P is present well below basal levels, losing its negative regulatory effect, which in turn mimics the effect of Sortin2 on cellular trafficking. By contrast, following Sortin2 treatment, increased levels of PI4P recruit proteins with relatively low affinity for PI4P that stimulate endocytic trafficking to the vacuole and LRP formation. Such interactors might be RAB proteins, as mentioned above, and/or other proteins whose identities and functions remain to be determined.

### Physiological Mechanisms of LR Organogenesis

The *pi4kiii $\beta$ 1 pi4kiii $\beta$ 2* mutant displays hormone-related phenotypes associated with the increased biosynthesis of salicylic acid (SA) and the constitutive expression of pathogenesis-related genes: stunted rosette growth and increased resistance to *Pseudomonas syringae* (Šašek et al., 2014). However, the major root phenotypes of the mutant (shorter roots and non-polarized root hairs) are not explained by an increase in SA levels (Šašek et al., 2014). Increased SA levels do not lead to the increased LRP and LR formation observed in the double mutant, since this hormone does not promote LR organogenesis. Furthermore, the LRP phenotype of *pi4kiii $\beta$ 1 pi4kiii $\beta$ 2* is not related to altered auxin levels or signaling, since it displays similar auxin levels and auxin-dependent gene expression to the wild-type line (Šašek et al., 2014).

The participation of the PI4KIII $\beta$ s reinforces the notion that endocytic trafficking is a distinct mechanism from TIR1/AFB-dependent LR organogenesis (Pérez-Henríquez et al., 2012). The *pi4kiii $\beta$ 1 pi4kiii $\beta$ 2* double mutant exhibited modified root system architecture in response to the auxin NAA, but not to Sortin2 (Fig. 4A). Consistently, the acute chemical inhibition of PI4KIII $\beta$ s in wild-type seedlings specifically affected LRP formation promoted by Sortin2 without affecting LRP formation controlled by the developmental program or auxin-induced LRP formation (Fig. 1A). These results indicate that at least two molecular mechanisms underlie root organogenesis. The known role of PI4P in endomembrane trafficking could explain the pivotal role of PI4KIII $\beta$ -dependent endocytosis in root organogenesis.

Finally, PI4P and other phosphoinositides function in various signaling processes (Ischebeck et al., 2010; Munnik and Vermeer, 2010; Delage et al., 2012). Perhaps PI4P is involved in transmitting environmental cues that promote root organogenesis independently of SCF<sup>TIR1/AFB</sup>. The flux of sugars influences plant development and physiology. The presence of Glc in the growth medium and mechanical stimulation increase the number of LRs, even in plants with a loss of function of the auxin receptor TIR1 (Mishra et al., 2009; Richter et al., 2009). Glc also promotes ligand-dependent endocytosis, resulting in the activation of signaling linking the developmental process to a protein-trafficking mechanism, although the roles of

PI4P and other PIs in this process remain unknown (Urano et al., 2012).

Overall, the findings presented here support the requirement of PIP4 and the enzymes PI4KIII $\beta$ 1 and PI4KIII $\beta$ 2 in the LRP formation induced by stimulation of endocytic trafficking, which is a mechanism that is independent of the auxin receptor complex SCF<sup>TIR1/AFB</sup>. Moreover, these enzymes function as negative regulators of constitutive LRP formation under normal plant growth conditions.

## MATERIALS AND METHODS

### Plant Material and Growth Conditions

*Arabidopsis* (*Arabidopsis thaliana*) wild-type ecotype Columbia-0, the double homozygous mutant *pi4kiii $\beta$ 1 pi4kiii $\beta$ 2* (SALK\_040479 SALK\_098069; Preuss et al., 2006), and the transgenic PI4P biosensor *Arabidopsis* line 35S:YFP-PHF<sup>FAPPI</sup> (Vermeer et al., 2009; Simon et al., 2014) were used in this study. Sterilized seeds were sown in solid culture medium (MSS) containing liquid culture medium (MSL) formulated with 0.5 $\times$  Murashige and Skoog salts (M519, PhytoTechnology Laboratories), 1% (w/v) Suc, 0.05% (w/v) MES (pH 5.7), and 0.01% (w/v) myo-inositol, and 0.7% (w/v) Phytoagar (PhytoTechnology Laboratories). The seedlings were grown vertically in MSS in growth chambers at 22°C under a 16-h-light/8-h-dark photoperiod.

### Chemical Treatments

Treatments were performed on MSL unless otherwise stated. Sortin2 (46 mM), PAO (60 mM), and NAA (10 mM) stocks were dissolved separately in 100% (v/v) DMSO. The final concentration of DMSO in all treatment and control conditions was 1% (v/v). Before seedling treatment, MSL containing Sortin2 (working concentrations of 14.5, 29, or 58  $\mu$ M Sortin2) was exposed to 6,200 lumens in a growth chamber under a 16-h-light/8-h-dark photoperiod for 4 d. To evaluate PI4P biosensor distribution and FM4-64 endocytosis under PI4K inhibition, 60-min pretreatments with 0.1 or 20  $\mu$ M PAO were performed. The same concentration of PAO was maintained during the assay. For chronic inhibition of PI4K activity, sterilized wild-type and *pi4kiii $\beta$ 1 pi4kiii $\beta$ 2* seeds were incubated on MSS supplemented with 0.1, 1, 10, or 20  $\mu$ M PAO for 10 d.

### LR Architecture

Seedlings were fixed in 70% (v/v) ethanol for 24 h and cleared for an additional 24 h with 90% (v/v) lactic acid. To analyze root architecture, seedlings were transferred to a microscope slide. Slides were scanned in an Epson V600 Scanner, and primary root length was measured. LRPs and eLRs were scored under a Nikon E200 light microscope (200 $\times$ ). The number of LRP and eLRs relative to the primary root length for each seedling was used as a measure of density. The beginning of the primary root differentiation zone was identified as the position where the first apical root hair appeared, and the most apical eLR delimited the FZ. The BZ was defined as the primary root section between the most apical eLR and the root-shoot transition zone (Dubrovsky and Forde, 2012).

### Endocytic Trafficking to the Vacuole

FM4-64 internalization was evaluated in epidermal root cells over time as described by Tejos et al. (2018). Seedlings were incubated in 5  $\mu$ M FM4-64 (Invitrogen) at 4°C for 5 min and transferred to 22°C before measuring FM4-64 internalization kinetics (time zero of internalization). Single confocal images were taken at 5, 30, 60, 90, and 120 min to evaluate FM4-64 localization under a Zeiss LSM 510 confocal microscope (laser 543 nm/emission > 560 nm, 1600 $\times$  zoom). Plasma membrane and intracellular FM4-64 signals were quantified using ImageJ v.1.49i. Selection of the region of interest (ROI) was performed manually for each cell.

The tracer FM1-43 (Bolte et al., 2004) was used to label the tonoplast. Seedlings were treated with 5  $\mu$ M FM1-43 (Invitrogen) for 10 min in MSL at 4°C and transferred to fresh MSL for 4 h in darkness at room temperature (22°C) to

allow for enrichment of the tracer in the tonoplast. Analysis of FM4-64 internalization was performed as described. Additionally, free FM4-64 was removed by washing the seedlings before analyzing FM4-64 internalization kinetics. Confocal single images from colabeled seedlings were captured under a Zeiss LSM 710 confocal microscope. FM1-43 and FM4-64 were detected by laser 488/ emission 533–568 nm and laser 543/ emission 588–696 nm, respectively. A FM4-64 fluorescence intensity map was constructed using LUT Rainbow RGB in ImageJ. The codistribution of FM1-43 and FM4-64 in the vacuole was analyzed using the Coloc2 and ICA plug-ins in FIJI. The ROI of the area occupied by the vacuole was selected manually in FM1-43–vacuole labeled cells.

## PI4P Level

The PI4P biosensor line 35S:YFP-PH<sup>FAPP1</sup> (Vermeer et al., 2009; Simon et al., 2014) was used to monitor the subcellular distribution of the PI4P biosensor in vivo. YFP fluorescence was evaluated under a Zeiss LSM 510 confocal microscope (laser 488/ emission 505–550 nm, 1600 $\times$  zoom). The recruitment of YFP-PH<sup>FAPP1</sup> to the membrane was quantified using the tool “Raw Integrated Density” of ImageJ v.1.49i (<http://fiji.sc/Fiji>). Selection of the ROI of the whole cell, plasma membrane, and intracellular space was performed by manually tracing single confocal images. The fluorescence from the whole cell (WC) and the intracellular space (IC) was quantified. The inner background cell fluorescence was considered to represent cytoplasmic fluorescence of the biosensor (Simon et al., 2014). The fluorescence intensity of the plasma membrane-localized biosensor was calculated by subtracting the IC fluorescent signal from the WC fluorescent signal. The recruitment of the biosensor to intracellular compartments was calculated by subtracting the inner background fluorescent signal from the IC fluorescent signal. The fluorescence intensity of the plasma membrane and intracellular compartments relative to WC fluorescence intensity was calculated to determine the recruitment to the membrane of each compartment. More detailed information can be found in the Supplemental Methods section.

## Rescue of the Defective Phenotype due to *PI4KIII $\beta$ 1* and *PI4KIII $\beta$ 2* Loss of Function

Purified PI4P (P-4016; Echelon Biosciences, Inc.) or PI3P (P-3016; Echelon Biosciences) was added to *pi4kiii $\beta$ 1 pi4kiii $\beta$ 2* seedlings following the manufacturer's protocol. Both PI4P and PI3P were dissolved to a final concentration of 522  $\mu$ M in chloroform:methanol:water (1:2:0.8). The protein carrier Carrier3 was dissolved to a concentration of 500  $\mu$ M in sterile water. Dissolved lipid and Carrier3 were incubated in a 1:1 M ratio for 45 min at 4°C. MSL containing 15  $\mu$ M:15  $\mu$ M lipid:Carrier3 was added to 5-d-old *pi4kiii $\beta$ 1 pi4kiii $\beta$ 2* seedlings. MSL containing an equivalent amount of chloroform:methanol:water solution and 15  $\mu$ M Carrier3 alone were used as controls to examine their effects on root system architecture parameters. The seedlings were grown for an additional of 5 d under these conditions.

## Accession Numbers

Sequence data from this article can be found in the GenBank/EMBL data libraries under accession numbers of AT5G64070 (*PI4KIII $\beta$ 1*) and AT5G09350 (*PI4KIII $\beta$ 2*).

## Supplemental Data

The following supplemental materials are available.

**Supplemental Methods.** Evaluation PI4P biosensor and root hair morphology.

**Supplemental Figure S1.** Treatment with 20  $\mu$ M PAO inhibits Sortin2-induced endocytic trafficking to the vacuole.

**Supplemental Figure S2.** PI4P biosensor distribution after Sortin2 exposure and during the inhibition of PI4K activity.

**Supplemental Figure S3.** LR architecture of the loss-of-function *pi4kiii $\beta$ 1 pi4kiii $\beta$ 2* mutant and its response to Sortin2, exogenous auxin, and PI4P.

**Supplemental Figure S4.** Inhibition of PI4K using 0.1  $\mu$ M PAO mimics the physiological and cellular phenotypes of the *pi4kiii $\beta$ 1* and *pi4kiii $\beta$ 2* loss-of-function mutant.

**Supplemental Figure S5.** Effect of PAO on endocytic trafficking in the *pi4kiii $\beta$ 1* and *pi4kiii $\beta$ 2* loss-of-function mutant.

## ACKNOWLEDGMENTS

We acknowledge Dr. Ricardo Tejos for scientific discussions and helpful advice and all members of the Norambuena team and Plant Molecular Biology Centre, Universidad de Chile for their helpful discussions of our work. We thank Carlos Salinas for reviewing the manuscript.

Received June 7, 2019; accepted June 17, 2019; published July 8, 2019.

## LITERATURE CITED

- Antignani V, Klocko AL, Bak G, Chandrasekaran SD, Dunivin T, Nielsen E (2015) Recruitment of PLANT U-BOX13 and the PI4K $\beta$ 1/ $\beta$ 2 phosphatidylinositol-4 kinases by the small GTPase RabA4B plays important roles during salicylic acid-mediated plant defense signaling in Arabidopsis. *Plant Cell* **27**: 243–261
- Beck M, Zhou J, Faulkner C, MacLean D, Robatzek S (2012) Spatio-temporal cellular dynamics of the Arabidopsis flagellin receptor reveal activation status-dependent endosomal sorting. *Plant Cell* **24**: 4205–4219
- Boerjan W, Cervera MT, Delarue M, Beeckman T, Dewitte W, Bellini C, Caboche M, Van Onckelen H, Van Montagu M, Inzé D (1995) Super-root, a recessive mutation in Arabidopsis, confers auxin overproduction. *Plant Cell* **7**: 1405–1419
- Bolte S, Talbot C, Boutte Y, Catrice O, Read ND, Satiat-Jeunemaitre B (2004) FM-dyes as experimental probes for dissecting vesicle trafficking in living plant cells. *J Microsc* **214**: 159–173
- Boss WF, Im YJ (2012) Phosphoinositide signaling. *Annu Rev Plant Biol* **63**: 409–429
- Casimiro I, Marchant A, Bhalerao RP, Beeckman T, Dhooge S, Swarup R, Graham N, Inzé D, Sandberg G, Casero PJ, Bennett M (2001) Auxin transport promotes Arabidopsis lateral root initiation. *Plant Cell* **13**: 843–852
- Delage E, Ruelland E, Guillas I, Zachowski A, Puyaubert J (2012) Arabidopsis type-III phosphatidylinositol 4-kinases  $\beta$ 1 and  $\beta$ 2 are upstream of the phospholipase C pathway triggered by cold exposure. *Plant Cell Physiol* **53**: 565–576
- De Rybel B, Vassileva V, Parizot B, Demeulenaere M, Grunewald W, Audenaert D, Van Campenhout J, Overvoorde P, Jansen L, Vanneste S, et al (2010) A novel aux/IAA28 signaling cascade activates GATA23-dependent specification of lateral root founder cell identity. *Curr Biol* **20**: 1697–1706
- Dharmasiri N, Dharmasiri S, Estelle M (2005) The F-box protein TIR1 is an auxin receptor. *Nature* **435**: 441–445
- Dubrovsky JG, Forde BG (2012) Quantitative analysis of lateral root development: Pitfalls and how to avoid them. *Plant Cell* **24**: 4–14
- Dubrovsky JG, Sauer M, Napsucially-Mendivil S, Ivanchenko MG, Friml J, Shishkova S, Celenza J, Benková E (2008) Auxin acts as a local morphogenetic trigger to specify lateral root founder cells. *Proc Natl Acad Sci USA* **105**: 8790–8794
- Ebine K, Inoue T, Ito J, Ito E, Uemura T, Goh T, Abe H, Sato K, Nakano A, Ueda T (2014) Plant vacuolar trafficking occurs through distinctly regulated pathways. *Curr Biol* **24**: 1375–1382
- Emans N, Zimmermann S, Fischer R (2002) Uptake of a fluorescent marker in plant cells is sensitive to brefeldin A and wortmannin. *Plant Cell* **14**: 71–86
- Fujimoto M, Suda Y, Vernhettes S, Nakano A, Ueda T (2015) Phosphatidylinositol 3-kinase and 4-kinase have distinct roles in intracellular trafficking of cellulose synthase complexes in *Arabidopsis thaliana*. *Plant Cell Physiol* **56**: 287–298
- Fukaki H, Nakao Y, Okushima Y, Theologis A, Tasaka M (2005) Tissue-specific expression of stabilized SOLITARY-ROOT/IAA14 alters lateral root development in Arabidopsis. *Plant J* **44**: 382–395
- Gruber BD, Giehl RFH, Friedel S, von Wirén N (2013) Plasticity of the Arabidopsis root system under nutrient deficiencies. *Plant Physiol* **163**: 161–179
- Heilmann I (2016) Phosphoinositide signaling in plant development. *Development* **143**: 2044–2055

- Heilmann M, Heilmann I (2015) Plant phosphoinositides-complex networks controlling growth and adaptation. *Biochim Biophys Acta* **1851**: 759–769
- Im YJ, Davis AJ, Perera IY, Johannes E, Allen NS, Boss WF (2007) The N-terminal membrane occupation and recognition nexus domain of Arabidopsis phosphatidylinositol phosphate kinase 1 regulates enzyme activity. *J Biol Chem* **282**: 5443–5452
- Ischebeck T, Seiler S, Heilmann I (2010) At the poles across kingdoms: Phosphoinositides and polar tip growth. *Protoplasma* **240**: 13–31
- Kang BH, Nielsen E, Preuss ML, Mastroratte D, Staehelin LA (2011) Electron tomography of RabA4b- and PI-4K $\beta$ 1-labeled trans Golgi network compartments in Arabidopsis. *Traffic* **12**: 313–329
- Kepinski S, Leyser O (2005) The Arabidopsis F-box protein TIR1 is an auxin receptor. *Nature* **435**: 446–451
- Kim DH, Eu YJ, Yoo CM, Kim YW, Pih KT, Jin JB, Kim SJ, Stenmark H, Hwang I (2001) Trafficking of phosphatidylinositol 3-phosphate from the trans-Golgi network to the lumen of the central vacuole in plant cells. *Plant Cell* **13**: 287–301
- Kolb C, Nagel MK, Kalinowska K, Hagmann J, Ichikawa M, Anzenberger F, Alkofer A, Sato MH, Braun P, Isono E (2015) FYVE1 is essential for vacuole biogenesis and intracellular trafficking in Arabidopsis. *Plant Physiol* **167**: 1361–1373
- König S, Ischebeck T, Lerche J, Stenzel I, Heilmann I (2008) Salt-stress-induced association of phosphatidylinositol 4,5-bisphosphate with clathrin-coated vesicles in plants. *Biochem J* **415**: 387–399
- Lee Y, Kim ES, Choi Y, Hwang I, Staiger CJ, Chung YY, Lee Y (2008) The Arabidopsis phosphatidylinositol 3-kinase is important for pollen development. *Plant Physiol* **147**: 1886–1897
- Li F, Chung T, Pennington JG, Federico ML, Kaeppler HF, Kaeppler SM, Otegui MS, Vierstra RD (2015) Autophagic recycling plays a central role in maize nitrogen remobilization. *Plant Cell* **27**: 1389–1408
- Lima JE, Kojima S, Takahashi H, von Wirén N (2010) Ammonium triggers lateral root branching in Arabidopsis in an AMMONIUM TRANSPORTER1; 3-dependent manner. *Plant Cell* **22**: 3621–3633
- Lin F, Krishnamoorthy P, Schubert V, Hause G, Heilmann M, Heilmann I (2019) A dual role for cell plate-associated PI4K $\beta$  in endocytosis and phragmoplast dynamics during plant somatic cytokinesis. *EMBO J* **38**: e100303
- Malamy JE, Benfey PN (1997) Organization and cell differentiation in lateral roots of *Arabidopsis thaliana*. *Development* **124**: 33–44
- Marhavý P, Vanstraelen M, De Rybel B, Zhaojun D, Bennett MJ, Beekman T, Benková E (2013) Auxin reflux between the endodermis and pericycle promotes lateral root initiation. *EMBO J* **32**: 149–158
- Matsuoka K, Bassham DC, Raikhel NV, Nakamura K (1995) Different sensitivity to wortmannin of two vacuolar sorting signals indicates the presence of distinct sorting machineries in tobacco cells. *J Cell Biol* **130**: 1307–1318
- Mishkind M, Vermeer JEM, Darwish E, Munnik T (2009) Heat stress activates phospholipase D and triggers PIP accumulation at the plasma membrane and nucleus. *Plant J* **60**: 10–21
- Mishra BS, Singh M, Aggrawal P, Laxmi A (2009) Glucose and auxin signaling interaction in controlling *Arabidopsis thaliana* seedlings root growth and development. *PLoS One* **4**: e4502
- Miura K, Lee J, Gong Q, Ma S, Jin JB, Yoo CY, Miura T, Sato A, Bohnert HJ, Hasegawa PM (2011) SIZ1 regulation of phosphate starvation-induced root architecture remodeling involves the control of auxin accumulation. *Plant Physiol* **155**: 1000–1012
- Mudgil Y, Shiu SH, Stone SL, Salt JN, Goring DR (2004) A large complement of the predicted Arabidopsis ARM repeat proteins are members of the U-box E3 ubiquitin ligase family. *Plant Physiol* **134**: 59–66
- Mueller-Roeber B, Pical C (2002) Inositol phospholipid metabolism in Arabidopsis. Characterized and putative isoforms of inositol phospholipid kinase and phosphoinositide-specific phospholipase C. *Plant Physiol* **130**: 22–46
- Munnik T, Nielsen E (2011) Green light for polyphosphoinositide signals in plants. *Curr Opin Plant Biol* **14**: 489–497
- Munnik T, Vermeer JEM (2010) Osmotic stress-induced phosphoinositide and inositol phosphate signalling in plants. *Plant Cell Environ* **33**: 655–669
- Okazaki K, Miyagishima SY, Wada H (2015) Phosphatidylinositol 4-phosphate negatively regulates chloroplast division in Arabidopsis. *Plant Cell* **27**: 663–674
- Okushima Y, Fukaki H, Onoda M, Theologis A, Tasaka M (2007) ARF7 and ARF19 regulate lateral root formation via direct activation of LBD/ASL genes in Arabidopsis. *Plant Cell* **19**: 118–130
- Pérez-Henríquez P, Raikhel NV, Norambuena L (2012) Endocytic trafficking towards the vacuole plays a key role in the auxin receptor SCF<sup>TIR1</sup>-independent mechanism of lateral root formation in *A. thaliana*. *Mol Plant* **5**: 1195–1209
- Pérez-Torres CA, López-Bucio J, Cruz-Ramírez A, Ibarra-Laclette E, Dharmasiri S, Estelle M, Herrera-Estrella L (2008) Phosphate availability alters lateral root development in Arabidopsis by modulating auxin sensitivity via a mechanism involving the TIR1 auxin receptor. *Plant Cell* **20**: 3258–3272
- Petricka JJ, Winter CM, Benfey PN (2012) Control of Arabidopsis root development. *Annu Rev Plant Biol* **63**: 563–590
- Preuss ML, Schmitz AJ, Thole JM, Bonner HKS, Otegui MS, Nielsen E (2006) A role for the RabA4b effector protein PI-4K $\beta$ 1 in polarized expansion of root hair cells in *Arabidopsis thaliana*. *J Cell Biol* **172**: 991–998
- Richter GL, Monshausen GB, Krol A, Gilroy S (2009) Mechanical stimuli modulate lateral root organogenesis. *Plant Physiol* **151**: 1855–1866
- Šašek V, Janda M, Delage E, Puyaubert J, Guivarc'h A, López Maseda E, Dobrev PI, Caius J, Bóka K, Valentová O, Burketová L, Zachowski A, et al (2014) Constitutive salicylic acid accumulation in pi4kIII $\beta$ 1 $\beta$ 2 Arabidopsis plants stunts rosette but not root growth. *New Phytol* **203**: 805–816
- Simon MLA, Platre MP, Assil S, van Wijk R, Chen WY, Chory J, Dreux M, Munnik T, Jaillais Y (2014) A multi-colour/multi-affinity marker set to visualize phosphoinositide dynamics in Arabidopsis. *Plant J* **77**: 322–337
- Simon MLA, Platre MP, Marqués-Bueno MM, Armengot L, Stanislas T, Bayle V, Caillaud MC, Jaillais Y (2016) A PtdIns(4)P-driven electrostatic field controls cell membrane identity and signalling in plants. *Nat Plants* **2**: 16089
- Tejos R, Sauer M, Vanneste S, Palacios-Gomez M, Li H, Heilmann M, van Wijk R, Vermeer JEM, Heilmann I, Munnik T, Friml J (2014) Bipolar plasma membrane distribution of phosphoinositides and their requirement for auxin-mediated cell polarity and patterning in Arabidopsis. *Plant Cell* **26**: 2114–2128
- Tejos R, Osorio-Navarro C, Norambuena L (2018) The use of drugs in the study of vacuole morphology and trafficking to the vacuole in *Arabidopsis thaliana*. In C Pereira, ed, *Plant Vacuolar Trafficking*, Vol 1789. Humana Press, New York, pp 143–154
- Thole JM, Nielsen E (2008) Phosphoinositides in plants: Novel functions in membrane trafficking. *Curr Opin Plant Biol* **11**: 620–631
- Urano D, Phan N, Jones JC, Yang J, Huang J, Grigston J, Taylor JP, Jones AM (2012) Endocytosis of the seven-transmembrane RGS1 protein activates G-protein-coupled signalling in Arabidopsis. *Nat Cell Biol* **14**: 1079–1088
- van Leeuwen W, Vermeer JEM, Gadella TWJ, Jr., Munnik T (2007) Visualization of phosphatidylinositol 4,5-bisphosphate in the plasma membrane of suspension-cultured tobacco BY-2 cells and whole Arabidopsis seedlings. *Plant J* **52**: 1014–1026
- Van Norman JM, Xuan W, Beekman T, Benfey PN (2013) To branch or not to branch: The role of pre-patterning in lateral root formation. *Development* **140**: 4301–4310
- Vásquez-Soto B, Manríquez N, Cruz-Amaya M, Zouhar J, Raikhel NV, Norambuena L (2015) Sortin2 enhances endocytic trafficking towards the vacuole in *Saccharomyces cerevisiae*. *Biol Res* **48**: 39
- Vermeer JEM, Thole JM, Goedhart J, Nielsen E, Munnik T, Gadella TWJ, Jr. (2009) Imaging phosphatidylinositol 4-phosphate dynamics in living plant cells. *Plant J* **57**: 356–372
- Xuan W, Audenaert D, Parizot B, Möller BK, Njo MF, De Rybel B, De Rop G, Van Isterdael G, Mähönen AP, Vanneste S, et al (2015) Root cap-derived auxin pre-patterns the longitudinal axis of the Arabidopsis root. *Curr Biol* **25**: 1381–1388
- Zheng J, Han SW, Rodriguez-Welsh MF, Rojas-Pierce M (2014) Homotypic vacuole fusion requires VTI11 and is regulated by phosphoinositides. *Mol Plant* **7**: 1026–1040
- Zolla G, Heimer YM, Barak S (2010) Mild salinity stimulates a stress-induced morphogenic response in *Arabidopsis thaliana* roots. *J Exp Bot* **61**: 211–224